ISA Transactions 52 (2013) 242–251

Contents lists available at SciVerse ScienceDirect

ISA Transactions

journal homepage: www.elsevier.com/locate/isatrans

A new control scheme for PID load frequency controller of single-area and multi-area power systems

Dola Gobinda Padhan *, Somanath Majhi

Department of Electronics and Electrical Engineering, Indian Institute of Technology Guwahati, Guwahati 781039, India

ARTICLE INFO

Article history:
Received 5 April 2012
Received in revised form
11 October 2012
Accepted 19 October 2012
Available online 7 November 2012
This paper was recommended for publication by Dr. Ahmad B. Rad.

Keywords:
LFC
PID
Laurent series
Disturbance rejection
Time delay
Relay feedback identification

ABSTRACT

A new control structure with a tuning method to design a PID load frequency controller for power systems is presented. Initially, the controller is designed for single area power system, then it is extended to multi-area case. The controller parameters are obtained by expanding controller transfer function using Laurent series. Relay based identification technique is adopted to estimate power system dynamics. Robustness studies on stability and performance are provided, with respect to uncertainties in the plant parameters. The proposed scheme ensures that overall system remains asymptotically stable for all bounded uncertainties and for system oscillations. Simulation results show the feasibility of the approach and the proposed method improves the load disturbance rejection performance significantly even in the presence of the uncertainties in plant parameters.

1. Introduction

The active power and frequency control is referred to as load frequency control (LFC) which has been used as an effective ancillary service in power systems for many years [1]. Several papers have been published to address the LFC [2–4]. For large scale power systems with interconnected areas, LFC is important to keep the system frequency and the inter-area tie-line power as near to the scheduled values as possible. In addition, the LFC has to be robust against unknown external disturbances and system model and parameter uncertainties. Many control strategies for load frequency control in power systems had been proposed by researchers over the past decades [5–21]. This extensive research is due to fact that LFC constitutes an important function of power system operation where the main objective is to regulate the output power of each generator at prescribed levels while keeping the frequency fluctuations within predetermined limits. Most of the reported works of the LFC problem have been tested for their robustness against large step load change. However, very few of the published researches deal with parameter uncertainties. In this paper, a design method for the LFC PID is proposed, which is able to consider uncertainties in power systems. Even though many advanced control theories have been established, most industrial controllers still use conventional applications such as PI or PID. PID controllers are preferred due to their simple structures, robustness, applicability over a wide range and easy in implementation on analog or digital platform [22]. We especially pay attention in modeling of the power system dynamics using relay feedback identification method and PID controller design for the developed model. In the proposed method, a Laurent series has been used in order to derive the expression for the controller's parameters. The proposed scheme leads to substantial control performance improvement, especially for the disturbance rejection. Simulation examples are provided to show the superiority of the proposed design method, compared with recently reported methods.

For clear interpretation, the proposed control structure is presented in Section 2. The modeling of power system dynamics, controller design, simulation results and robustness analysis for single area power system are given in Section 3. Multi-area power system is addressed in Section 4 followed by the conclusions in Section 5.

2. Proposed control structure

The proposed control structure for LFC is shown in Fig. 1 which has only one controller (G_c). Unlike the conventional LFC control

* Corresponding author. Tel.: +91 361 2582508; fax: +91 361 2690762.
E-mail addresses: dola@iitg.ernet.in (D.G. Padhan), smajhi@iitg.ernet.in (S. Majhi).

0019-0578/$ - see front matter © 2012 ISA. Published by Elsevier Ltd. All rights reserved.
http://dx.doi.org/10.1016/j.isatra.2012.10.003

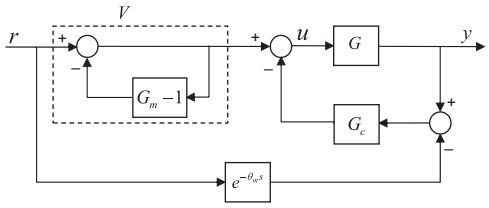

Fig. 1. Proposed control structure.

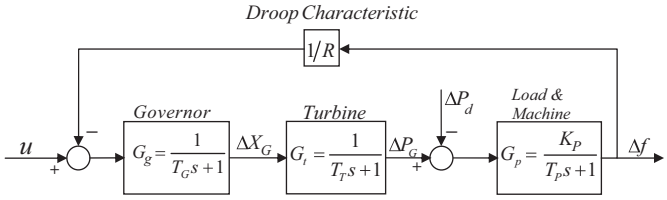

Fig. 2. Block diagram of a single-area power system.

structure, the proposed structure uses the controller G_c in the feedback path. Although, G_c is primarily meant for load disturbance rejection, it also takes part in stabilizing the oscillatory process in the loop. G represents the transfer function of overall plant. θ_m is the time delay part and G_m is the transfer function of the delay free part of the plant model.

The closed-loop transfer function relating the output (y) to the reference (r) can be written as

$$\frac{y}{r} = \frac{G + GG_cG_me^{-\theta_m s}}{G_m(1+GG_c)} \tag{1}$$

When the model used exactly matches the plant dynamics, (1) reduces to

$$\frac{y}{r} = e^{-\theta_m s} \tag{2}$$

this indicates the system output can reach the setpoint value just after the process time delay. It is to be noted that the block V primarily helps in improving the overall servo performance of the closed-loop system. It is popularly known that for LFC design, the load disturbance rejection is more important than the setpoint response [15]. Therefore, the controller G_c has been designed mainly for power system load disturbances.

3. Single area power system

3.1. Modeling of power system dynamics

A linear model of a single-area power system is shown in Fig 2, in which a single generator is supplying power to a single-area. In the present work, non-reheat turbine (NRT) and reheat turbine (RT) are considered for LFC modeling. The plant model used for LFC without droop characteristics is

$$G = G_gG_tG_p \tag{3}$$

where G_g, G_t and G_p are the dynamics of the governor, turbine and load&machine, respectively. The governor dynamics $G_g = 1/(T_Gs+1)$ and the Load and machine dynamics, $G_p = K_p/(T_ps+1)$. Non-reheat turbines are first-order units. The dynamics of the non-reheat turbine is represented as $G_t = 1/(T_Ts+1)$. Reheat turbines are modeled as second-order units, since they have different stages due to high and low steam pressure. The transfer function of the reheat turbine is in the form of $G_t = (cT_rs+1)/(T_rs+1)(T_Ts+1)$ where T_r stands for the low pressure reheat time and c is the portion of the power generated by the reheat turbine in the total generated power.

The plant model used for LFC with droop characteristic is

$$G = \frac{G_gG_tG_p}{1+G_gG_tG_p/R} \tag{4}$$

For LFC, G generally results in higher order plant models which may be inconvenient for controller design. There are many process identification techniques suggested by various researchers [23–25]. In control theory, Majhi [26] introduces a relay based identification method for reducing a higher order process dynamics to a low order dynamics with time delay. This technique has been modified and applied for the first time in power systems to design a new PID load frequency controller for single-area and multi-area power system. Therefore, these higher order models are approximated by lower order transfer functions with time delay using relay based identification method [26]. Eqs. (3) and (4) can be represented by the second order transfer function model

$$G = \frac{ke^{-\theta_m s}}{(T_1s+1)(T_2s+1)} \tag{5}$$

Its state space equations in the Jordan canonical form become

$$\dot{x}(t) = Ax(t) + bu(t-\theta_m) \tag{6}$$

$$y(t) = cx(t) \tag{7}$$

where

$$A = \begin{bmatrix} \frac{-1}{T_1} & 0 \\ 0 & \frac{-1}{T_2} \end{bmatrix}, \quad b = \begin{bmatrix} 1 \\ 1 \end{bmatrix}, \quad c = \frac{k}{T_1 - T_2}[1 \ \ -1]$$

when a relay test is performed with a symmetrical relay of height $\pm h$, then the expression for the limit cycle output for $0 \le t \le \theta_m$ is

$$y(t) = ce^{At}x(0) + cA^{-1}(e^{At} - I)bh \tag{8}$$

Let the half period of the limit cycle output be τ. Then the expression for the limit cycle output for $\theta_m \le t \le \tau$ is

$$y(t) = ce^{A(t-\theta_m)}x(\theta_m) - cA^{-1}(e^{A(t-\theta_m)} - I)bh \tag{9}$$

The condition for a limit cycle output can be written as

$$y(0) = cx(0) = -y(\tau) = 0 \tag{10}$$

Substitution of $t = \tau$ in (9) and use of (8) gives the initial value of the cycling states

$$x(0) = (I + e^{A\tau})^{-1}A^{-1}(2e^{A(\tau-\theta_m)} - e^{A\tau} - I)bh \tag{11}$$

When t_p is the time instant at which the positive peak output occurs and $t_p \ge \theta_m$, then the expression of the peak output A_p becomes

$$A_p = c(e^{A(t_p-\theta_m)}x(\theta_m) - A^{-1}(e^{A(t_p-\theta_m)} - I)bh) \tag{12}$$

and the expression for the peak time becomes

$$t_p = \theta_m + \frac{T_1T_2}{T_1 - T_2}\ln\left(\frac{1+e^{-\tau/T_1}}{1+e^{-\tau/T_2}}\right) \tag{13}$$

Substitution of A, b and c in (11) and (12) gives

$$T_1(1+e^{-\tau/T_2})(2e^{-(\tau-\theta_m)/T_1} - e^{-\tau/T_1} - 1) - T_2(1+e^{-\tau/T_1}) \times (2e^{-(\tau-\theta_m)/T_2} - e^{-\tau/T_2} - 1) = 0 \tag{14}$$

$$A_p = kh(2(1+e^{-\tau/T_1})^{-T_1/(T_1-T_2)}(1+e^{-\tau/T_2})^{T_2/(T_1-T_2)} - 1) \tag{15}$$

Eqs. (13)–(15) are solved simultaneously to estimate θ_m, T_1 and T_2 from the measurements of τ, A_p and t_p. The steady state gain k is assumed to be known a priori or can be estimated from a step signal test. Care has been taken to solve the set of non-linear equations so that convergence may not take place to a false solution.

3.2. Design of the controller G_c

For easy implementation of PID controller, G_c is considered in the following form:

$$G_c = K_c\left(1+\frac{1}{T_i s}+\frac{T_d s}{\varepsilon T_d s+1}\right) \tag{16}$$

where the derivative filter constant is typically fixed by the manufacture [27] and $\varepsilon=0.1$ throughout the paper. In the proposed control structure shown in Fig. 1, the nominal complementary sensitivity function for load disturbance rejection can be obtained as

$$T = \frac{GG_c}{1+GG_c} \tag{17}$$

In order to reject a step change in load of power system, the asymptotic constraint

$$\lim_{s\to -\frac{1}{T_1},-\frac{1}{T_2}} (1-T) = 0 \tag{18}$$

should be satisfied so that the closed-loop internal stability can be achieved. The desired closed-loop complementary sensitivity function is proposed as

$$T = \frac{(\alpha_2 s^2+\alpha_1 s+1)}{(\lambda s+1)^4} e^{-\theta_m s} \tag{19}$$

where λ is a tuning parameter for obtaining the desirable performance of the power system. α_1 and α_2 can be obtained from (18) and (19) as $\alpha_1 = (T_1^2((1-\lambda/T_1)^4 e^{-\theta_m/T_1}-1)-T_2^2((1-\lambda/T_2)^4 e^{-\theta_m/T_2}-1))/(T_2-T_1)$ and $\alpha_2 = T_2^2((1-\lambda/T_2)^4 e^{-\theta_m/T_2}-1)+T_2\alpha_1$. Using (17) and (19), we get

$$G_c = \frac{(T_1 s+1)(T_2 s+1)(\alpha_2 s^2+\alpha_1 s+1)}{k[(\lambda s+1)^4 - e^{-\theta_m s}(\alpha_2 s^2+\alpha_1 s+1)]} \tag{20}$$

The resulting controller G_c does not have a standard PID controller form. Therefore, in order to produce the desired disturbance rejection controller, the following procedure is employed. G_c can be approximated by an approximation series in a complex plane, by expanding it near vicinity of zero. Laurent series has been used for approximation instead of Taylor or MacLaurin series (where terms with s^0, s^1, and s^2 appear), Laurent series has been chosen (because the controller is given by (16), where terms with s^0, s^{-1}, and s^1 appear, the series no longer belongs to the Taylor or Maclaurin type, but becomes Laurent type, with other coefficients as zeros) because it addresses complex coefficients that are important especially to investigate the behavior of functions near singularity. A practical desired disturbance rejection controller should possess an integral characteristic to eliminate any system output deviation arising from load disturbances. Therefore, let

$$G_c = \frac{f(s)}{s} \tag{21}$$

or

$$G_c = \frac{\gamma(s)}{s(1+\beta s)} \tag{22}$$

Now, expanding G_c in the vicinity of zero by Laurent series

$$G_c = \frac{1}{s(\beta s+1)}\left(\cdots+\gamma(0)+\gamma'(0)s+\frac{\gamma''(0)s^2}{2!}+\cdots\right) \tag{23}$$

The parameters of G_c obtained from (16) and (23)

$$\begin{cases} K_c = \gamma'(0) \\ \dfrac{K_c}{T_i} = \gamma(0) \\ K_c T_d = \dfrac{\gamma''(0)}{2!} \end{cases} \tag{24}$$

where $\gamma(0)=f(0)$, $\gamma'(0)=\beta f(0)+f'(0)$, $\gamma''(0)=2\beta f'(0)+f''(0)$, $f(0)=1/k(4\lambda-\alpha_1+\theta_m)$,

$$f'(0) = \frac{T_1\theta_m+T_2\theta_m+(\theta_m^2/2)-T_2\alpha_1+4\alpha_1\lambda-\alpha_1^2+\alpha_2+4T_1\lambda-T_1\alpha_1-6\lambda^2+4T_2\lambda}{k(16\lambda^2-8\alpha_1\lambda+8\theta_m\lambda+\alpha_1^2-2\theta_m\alpha_1+\theta_m^2)}$$

and

$$f''(0) = \frac{\begin{pmatrix} 48\theta_m\alpha_2\lambda+72\theta_m\alpha_1\lambda^2-24\theta_m\alpha_2\alpha_1+48\theta_m^2\alpha_1\lambda+24T_2\lambda\theta_m^2 \\ +48T_2\lambda\alpha_2+6T_2\theta_m^3+48\alpha_2\lambda^2 \\ +48T_2\lambda\theta_m\alpha_1-12T_2\alpha_2\alpha_1+264T_1\lambda^2\alpha_1-24T_1T_2\alpha_1\theta_m \\ -96T_1\alpha_1^2\lambda+24T_1\lambda\theta_m^2+48T_1\lambda\alpha_2 \\ +12T_1T_2\theta_m^2+48T_1\lambda\theta_m\alpha_1+12T_1T_2\alpha_1^2+96T_1T_2\theta_m\lambda \\ +192T_1T_2\lambda^2-72T_2\lambda^2\theta_m-96T_2\alpha_1^2\lambda \\ -96T_1T_2\alpha_1\lambda-48\theta_m\alpha_1^2\lambda+6T_1\theta_m^3-48\alpha_2\lambda\alpha_1+264T_2\lambda^2\alpha_1 \\ +12T_2\alpha_1^3+12\theta_m\alpha_1^3+12\alpha_2^2 \\ +\theta_m^4-12T_1\alpha_2\alpha_1+12T_2\theta_m\alpha_2-288T_2\lambda^3-288T_1\lambda^3 \\ -240\alpha_1\lambda^3+12T_1\theta_m\alpha_2+12T_1\alpha_1^3 \\ -72\theta_m^2\lambda^2-48\theta_m\lambda^3-12\theta_m^2\alpha_1^2+240\lambda^4-6T_2\theta_m^2\alpha_1 \\ -6T_1\theta_m^2\alpha_1-12T_1\theta_m\alpha_1^2+72\lambda^2\alpha 1^2 \\ -72T_1\lambda^2\theta_m-8\theta_m^3\lambda+2\theta_m^3\alpha_1+12\theta_m^2\alpha_2-12T_2\theta_m\alpha_1^2 \end{pmatrix}}{\begin{pmatrix} 384k\lambda^3-288k\alpha_1\lambda^2+288k\theta_m\lambda^2+72k\lambda\alpha_1^2 \\ -144k\lambda\theta_m\alpha_1+72k\theta_m^2\lambda-6k\alpha_1^3 \\ +18k\theta_m\alpha_1^2-18k\theta_m^2\alpha_1+6k\theta_m^3 \end{pmatrix}}$$

Thus, K_c, T_i and T_d can be obtained from (24).

3.3. Simulation results for single area power system

Example 1. Consider a power system with a non-reheated turbine and a reheated turbine studied by Tan [17]. The model parameters are

Non-reheated turbine: $K_P=120$, $T_P=20$, $T_T=0.3$, $T_G=0.08$, $R=2.4$.
Reheated turbine: $K_P=120$, $T_P=20$, $T_T=0.3$, $T_G=0.08$, $R=2.4$, $T_r=4.2$ and $c=0.35$.

The Nyquist plots of the identified and actual models for the non-reheat turbine without droop (NRTWD) are shown in Fig. 3 to illustrate the accuracy of the identification method. By selecting suitable value of λ and β, the controller settings (see Table 1)

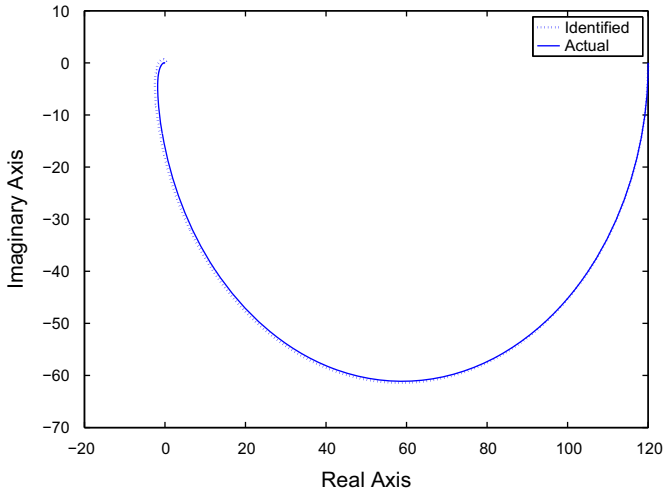

Fig. 3. Nyquist plots for the power system with NRTWD for example-1.

Table 1

	Identified model	Controller parameters
NRTWD	$\frac{120e^{-0.4626s}}{(28.4952s+1)(0.2202s+1)}$	$K_c=1.0326, T_i=1.2116, T_d=0.3420$
NRTD	$\frac{250e^{-0.05s}}{2.028s^2+12.765s+106.2}$	$K_c=1.4978, T_i=1.1481, T_d=0.1574$
RTWD	$\frac{120e^{-0.541s}}{(23.2137s+1)(0.9057s+1)}$	$K_c=3.6317, T_i=1.0998, T_d=0.4828$
RTD	$\frac{235.3e^{-0.035s}}{1.79s^2+16.9s+100}$	$K_c=6.164, T_i=3.1934, T_d=0.1882$

NRTWD, non-reheat turbine without droop; NRTD, non-reheat turbine with droop; RTWD, reheat turbine without droop; RTD, reheat turbine with droop.

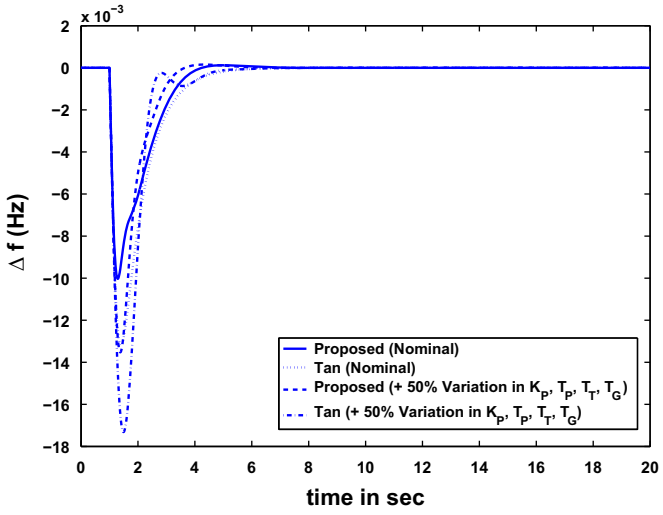

Fig. 4. Frequency deviation for NRTWD.

for the power system with non-reheated and reheated turbines can be obtained using (24). By the help of extensive simulation study, $\lambda=0.13$ and $\beta=0.012$ for NRTWD, $\lambda=0.11$ and $\beta=1$ for NRTD, $\lambda=0.05$ and $\beta=0.0035$ for RTWD and $\lambda=0.1$ and $\beta=3$ for RTD. Figs. 4–7 show the frequency changes of the power system following a load demand $\Delta P_d=0.01$. The stability robustness is tested by changing the parameters (K_P, T_P, T_T, T_G) of the system by $\pm 50\%$. From the simulation results, it is evident that the proposed method gives improved performance than Tan's method.

Example 2. Consider a power system with a non-reheated turbine studied by Khodabakhshian and Edrisi [15]. The model parameters are $K_P=1.25$, $T_P=12.5$, $T_T=0.5$, $T_G=0.2$, $R=0.05$.

The Nyquist plots of the identified and actual models are shown in Fig. 8 to illustrate the accuracy of the identification method. The PID controller parameters in the case of Khodabakhshian and Edrisi are $T_d=0.01$, $K_p=36.22$, $K_i=2.77$ and $K_d=19.6$. For the proposed method, the controller parameters are obtained as $K_c=55.2051$, $T_i=1.1797$, $T_d=0.5173$ by choosing $\lambda=0.19$ and $\beta=0.3$. With these controller settings, a load demand $\Delta P_d=0.02$ is introduced at $t=1$ s. The corresponding frequency deviations are shown in Fig. 9. Now, to test the robustness of the systems, -20% variation in T_P and $+10\%$ variation in K_P have been considered simultaneously. The frequency deviations for perturbed systems are given in Fig. 10. From the simulation results, it is clear that the proposed method gives smaller undershoot and settling time than Khodabakhshian and Edrisi's method.

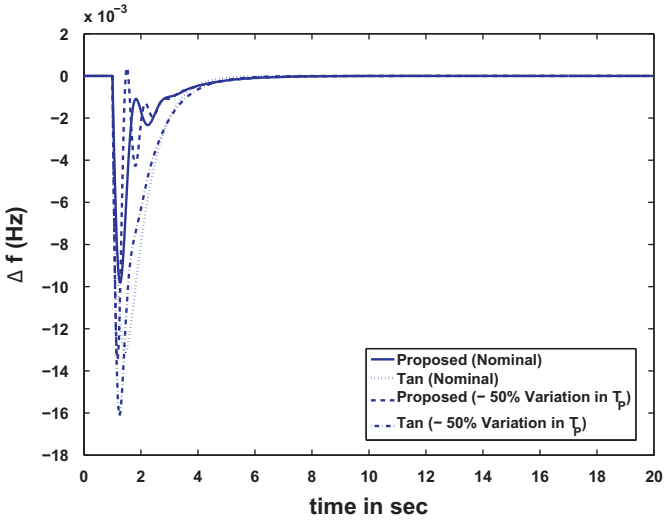

Fig. 5. Frequency deviation for NRTD.

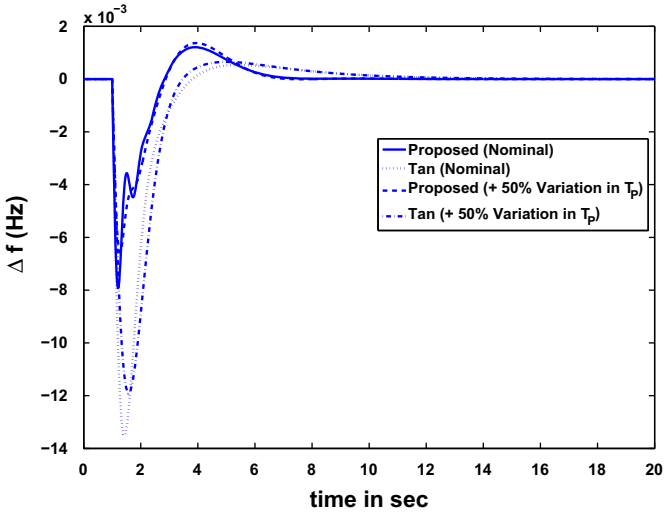

Fig. 6. Frequency deviation for RTWD.

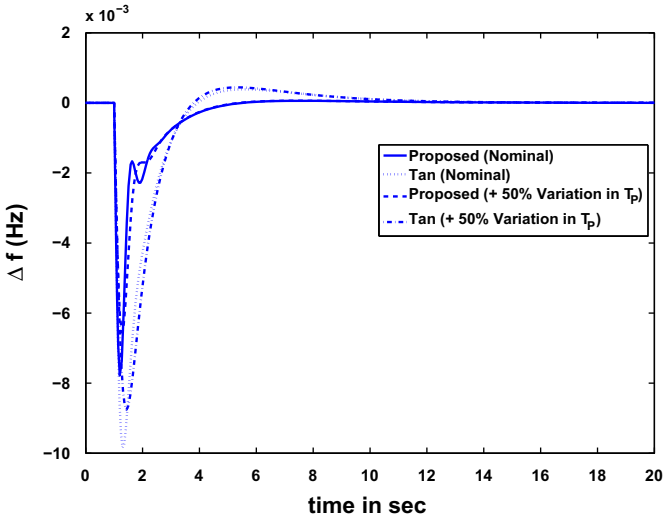

Fig. 7. Frequency deviation for RTD.

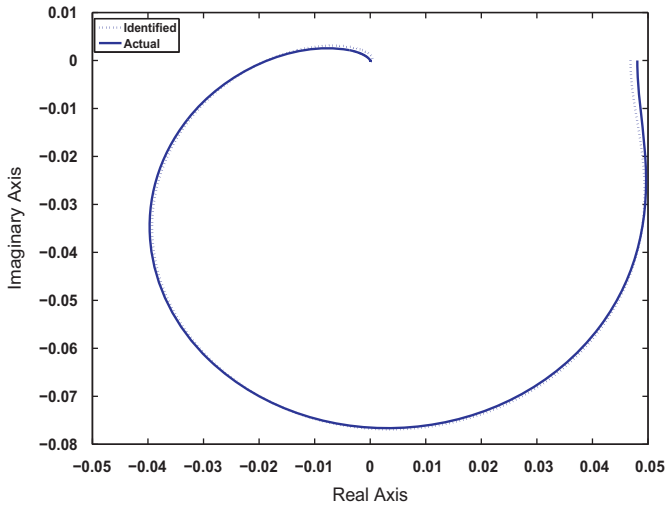

Fig. 8. Nyquist plots for the power system with NRTD for example-2.

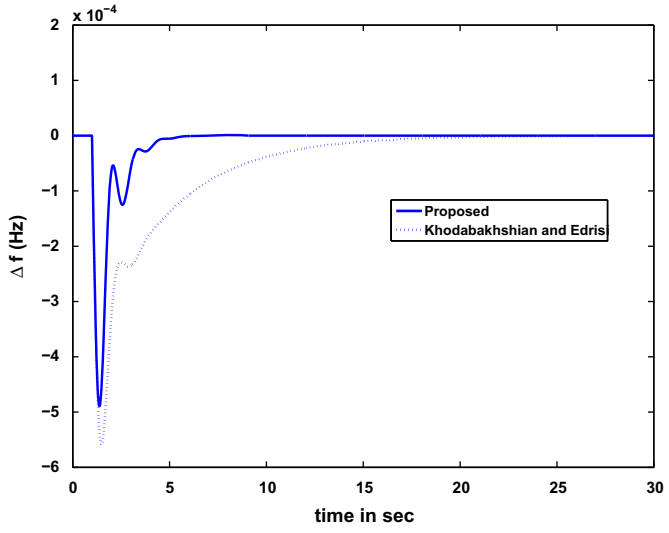

Fig. 9. Frequency deviations for nominal systems.

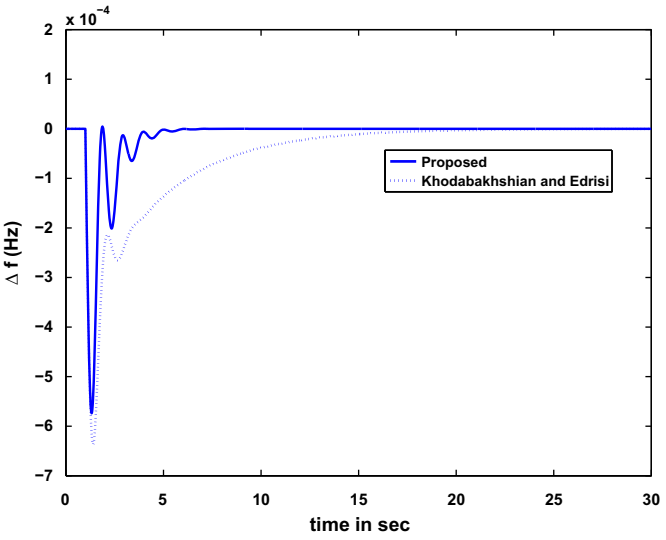

Fig. 10. Frequency deviations for perturbed systems.

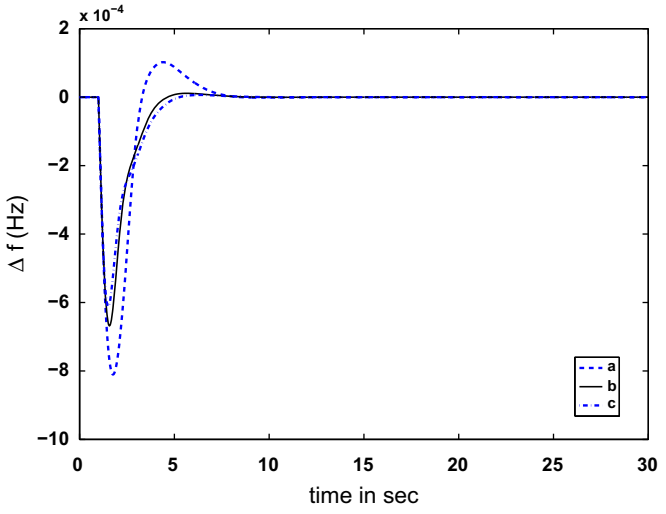

Fig. 11. Impact of saturation on frequency deviations: saturation limit (a) 0.03, (b) 0.04 and (c) 0.05.

3.4. Impact of saturation, windup and derivative kick

Consider the case of a power system with a non-reheated turbine without droop characteristic. The model parameters are same as that of example-2. For the proposed method, in order to get satisfactory closed-loop responses, the controller parameters are considered as K_c=41.2454, T_i=1.7243, T_d=0.4889. With an actuator saturation non-linear element given by saturation limits 0.03, 0.04 and 0.05, the related responses of the system are shown in Figs. 11 and 12. When there is an initial load change, the error signal is initially so large that the control signal quickly reaches its actuator saturation limit. Even when the output signal reaches the reference value, which gives a negative error signal due to the large value of the integrator output. The control signal still remains at the saturation value, which causes the output of the system to continuously increase until the negative action of the error signal begins to have effect. This phenomenon is referred to as the integrator windup action, which is undesirable in control applications.

When the output saturates, the integral is recomputed so that its new value gives an output at the saturation limit. The rate at which the controller output is reset is governed by the feedback gain, $1/T_t$, where T_t can be interpreted as the time constant (tracking time constant), which determines how quickly the integral is reset. When introducing anti-windup in power systems with derivative action, some care must be taken. If T_t is chosen too small, the errors can cause saturation of the output, which accidentally resets the integrator. T_t should be larger than T_d and smaller than T_i. For different T_t, the output signals are compared in Fig. 13. It can be seen that for smaller values of T_t, the windup phenomenon can be reduced more significantly.

In industrial applications, the pure derivative action is never used, due to the derivative kick produced in the control signal and to the undesirable noise amplification. It is usually cascaded by a first-order low pass filter. The effect of derivative filter on frequency deviations and control signals are shown in Figs. 14 and 15, respectively.

3.5. Robustness analysis

A study of robustness analysis is an important task in control system design because the behaviour of the real system is almost always different from the behavior of the model. The notion of robustness expresses the capability of a system to be insensitive to the effects of parameters variability. From (1), it is observed

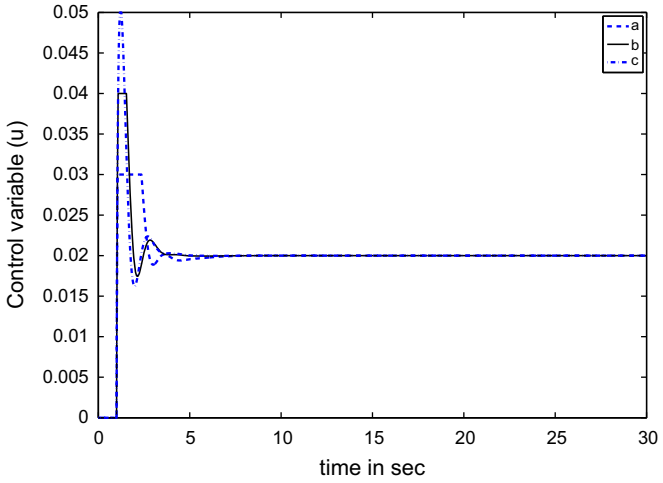

Fig. 12. Impact of saturation on control efforts: saturation limit (a) 0.03, (b) 0.04 and (c) 0.05.

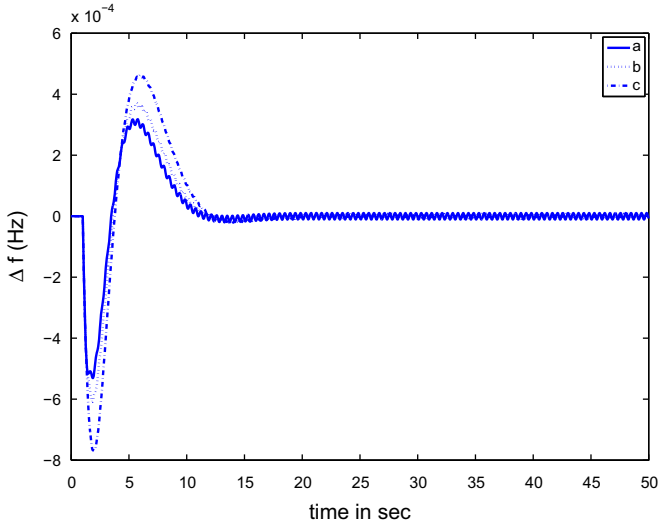

Fig. 13. Effect of tracking time on frequency deviations: (a) 10 s, (b) 6 s and (c) 1 s.

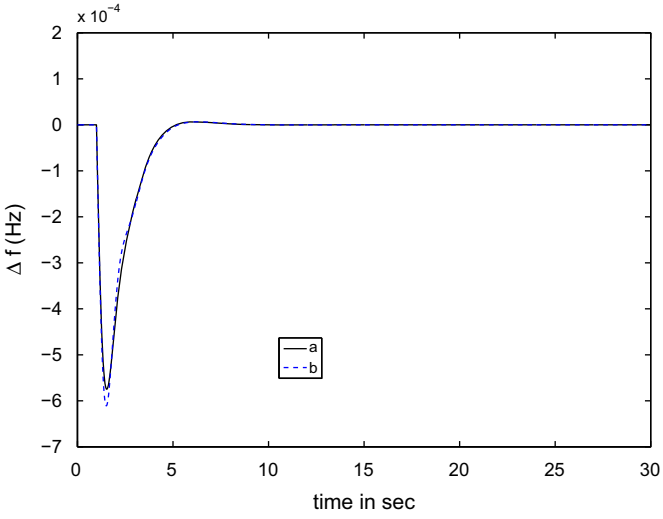

Fig. 14. Frequency deviations: (a) with derivative filter and (b) without derivative filter.

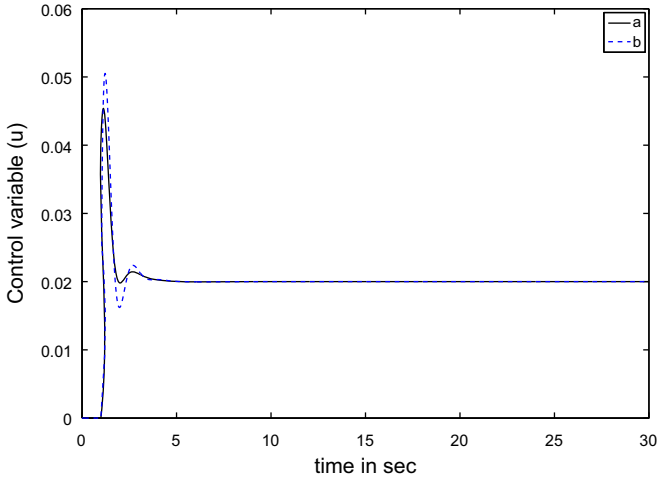

Fig. 15. Control efforts: (a) with derivative filter and (b) without derivative filter.

that the robust control performances can be studied by analyzing G_c as it affects the process model G in a single feedback path. The type of uncertainties affecting the design of G_c are the parametric uncertainties such as uncertainty in process gain, time constant and time delay.

According to the Small gain theorem [28], the closed loop system for the load disturbance rejection is robustly stable if and only if

$$\|\Delta_m(s)T(s)\|_\infty < 1 \tag{25}$$

where $T(s)$ is the closed loop complementary sensitivity function and $\Delta_m(s)$ is the process multiplicative uncertainty i.e. $\Delta_m(s) = |(G(s)-\tilde{G}_m(s))/\tilde{G}_m(s)|$ where $\tilde{G}_m(s) = G_m(s)e^{-\theta_m s}$. In order to show the robustness analysis more qualitatively, consider the process for which the closed-loop complementary sensitivity function is

$$T = \frac{kK_c(1+T_is+T_iT_d(1+\varepsilon)s^2)e^{-\theta_m s}}{(1+(T_1+T_2)s+T_1T_2s^2)(T_is+\varepsilon T_iT_ds^2)+kK_c(1+T_is+T_iT_d(1+\varepsilon)s^2)e^{-\theta_m s}} \tag{26}$$

where the controller parameters K_c, T_i and T_d are functions of the tuning parameters λ. Now, substituting (19) into (25) yields the robust stability constraint

$$\left\| \frac{\alpha_2 s^2+\alpha_1 s+1}{(\lambda s+1)^4} \right\|_\infty < \frac{1}{\|\Delta_m(s)\|_\infty} \tag{27}$$

for the control structure. where $\Delta_m(s)$ is the multiplicative uncertainty bound of the process G. For the process gain uncertainty, the tuning parameter should be selected in such a way that

$$\frac{(\omega^2\lambda^2+1)^2}{\sqrt{\omega^2\alpha_1^2+(1-\alpha_2\omega^2)^2}} > \frac{|\Delta k|}{k}, \quad \forall\omega > 0 \tag{28}$$

For the process time delay uncertainty $\Delta\theta_m$, the robust stability constraint for tuning λ is

$$\frac{\sqrt{\omega^2\alpha_1^2+(1-\alpha_2\omega^2)^2}}{(\omega^2\lambda^2+1)^2} < \frac{1}{|e^{-j\Delta\theta_m s}-1|}, \quad \forall\omega > 0 \tag{29}$$

If uncertainty exists in both process gain and time delay, the tuning parameter should be selected in such a way that

$$\frac{(\omega^2\lambda^2+1)^2}{\sqrt{\omega^2\alpha_1^2+(1-\alpha_2\omega^2)^2}} > \left| \left(1+\frac{\Delta k}{k}\right)e^{-j\Delta\theta_m\omega}-1 \right|, \quad \forall\omega > 0 \tag{30}$$

If the uncertainty exists in the parameters α_1 and α_2 then, by similar analysis, the value of λ should satisfy the following

constraint:

$$\|T(j\omega)\|_\infty < \left|\frac{\alpha_2 s^2+\alpha_1 s+1}{\Delta\alpha_2 s^2+\Delta\alpha_1 s+1}\right| \tag{31}$$

According to robust control theory [29], the closed-loop performance for load disturbance rejection is robust, the following constraints have to be followed by the sensitivity and complementary sensitivity functions:

$$\|\Delta_m(s)T(s)+w_1(s)(1-T(s))\| < 1 \tag{32}$$

where $w_1(s)$ is the weight function of the sensitivity function, $S(s)=1-T(s)$. Therefore, the tuning parameter λ should be selected such that the resulting controller satisfy the robust performance and robust stability constraints.

When modeling a high-order power systems, the model and parameter approximations cannot be avoided. A study of robustness analysis is an important task in LFC design because no mathematical model of a system will be a perfect representation of the actual system. If the controller tuning is too tight, the closed-loop system may become unstable with a small mismatch in the system parameters. Now, we will examine the closed-loop stability property of the proposed controller design with some mismatch in the plant parameters. Kharitonov's theorem is the well-known and simplest tool for robust stability analysis [30,31]. This theorem has been used for the robustness analysis considering parametric uncertainties in the plant parameters. The family of polynomials

$$P=\{p(s,q): q\in Q\} \tag{33}$$

is a set of polynomials $p(s,q)$ such that the uncertainty parameter q is an element of the uncertainty space Q. For a Q, the family is an interval polynomial family

$$\sum_{i=0}^{n} p(s,q)=\sum_{i=0}^{n} x_i s^i \triangleq \sum_{i=0}^{n}[l_i,h_i]s^i \tag{34}$$

where $x_i=[l_i,h_i]$ is an interval with an infinite set of x_i regarding $l_i<x_i<h_i$. According to the Kharitonov's theorem, an nth degree interval polynomial family is robustly stable if and only if each of the four Kharitonov polynomials are Hurwitz stable and value sets move in a anti-clockwise sense through n quadrants of the complex plane without passing through or touching the origin of the plane. A polynomial is Hurwitz stable if all roots are located in the left half of complex plane which is checked with the help of Routh criterion.

Table 2
The roots of Kharitonov polynomials for NRTWD.

$K_1(s)$	$K_2(s)$	$K_3(s)$	$K_4(s)$
$-0.56+j0.8632$	-0.9119	$-0.1682+j0.4189$	-1.602
$-0.56-j0.8632$	-0.292	$-0.1682+j0.4189$	-0.6671
-0.702	$-0.0131+j0.1537$	$-0.1628+j0.0614$	$-0.0063+j0.0743$
$-0.0318+j0.0332$	$-0.0131-j0.1537$	$-0.1628-j0.0614$	$-0.0063+j0.0743$
$-0.0318-j0.0332$	-0.0253	-0.014	-0.0502

Table 3
The roots of Kharitonov polynomials for NRTD.

$K_1(s)$	$K_2(s)$	$K_3(s)$	$K_4(s)$
-1.0912	-1.3406	-0.7835	-1.9953
$-0.161+j0.1225$	$-0.0044+j0.1417$	$-0.054+j0.2093$	-0.1495
$-0.161-j0.1225$	$-0.0044-j0.1417$	$-0.054+j0.2093$	$-0.032+j0.092$
-0.0575	-0.1259	-0.0919	$-0.032-j0.092$
-0.0188	-0.0142	-0.0096	-0.0255

The four Kharoitonov polynomials are given by

$$K_1(s)=h_0+l_1 s+l_2 s^2+h_3 s^3+h_4 s^4+l_5 s^5+l_6 s^6+h_7 s^7+\cdots$$

$$K_2(s)=h_0+h_1 s+l_2 s^2+l_3 s^3+h_4 s^4+h_5 s^5+l_6 s^6+l_7 s^7+\cdots$$

$$K_3(s)=l_0+h_1 s+h_2 s^2+l_3 s^3+l_4 s^4+h_5 s^5+h_6 s^6+l_7 s^7+\cdots$$

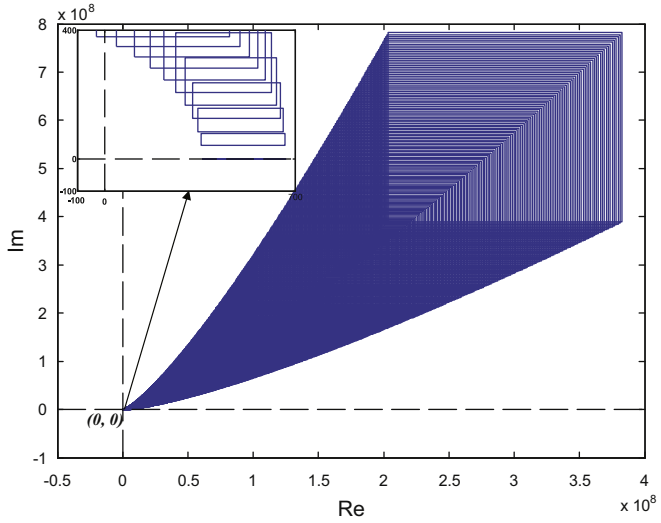

Fig. 16. Kharitonov's rectangles for the NRTWD.

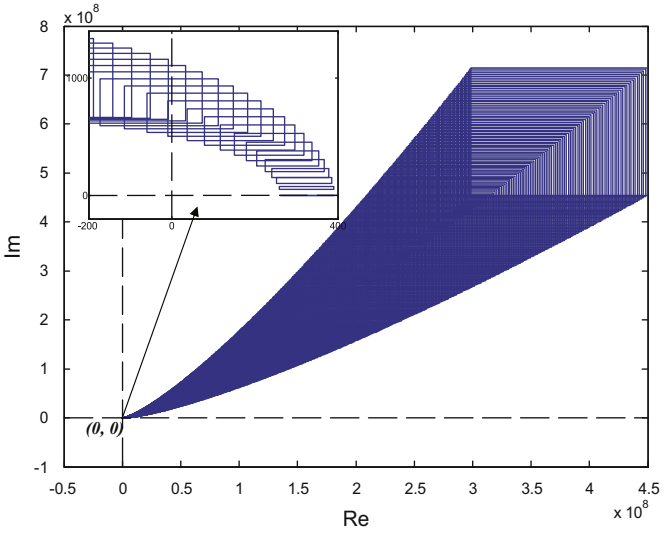

Fig. 17. Kharitonov's rectangles for the NRTD.

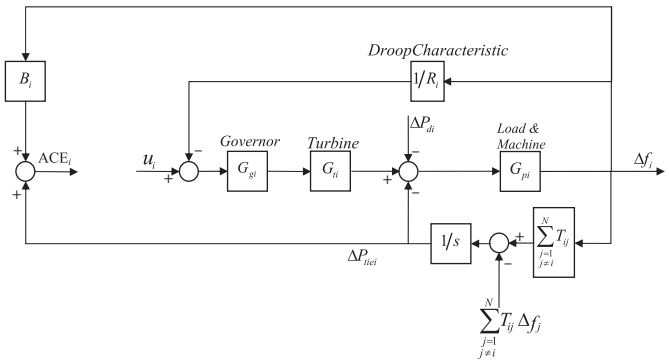

Fig. 18. Block diagram representation of control area i.

$$K_4(s) = l_0 + l_1 s + h_2 s^2 + h_3 s^3 + l_4 s^4 + l_5 s^5 + h_6 s^6 + h_7 s^7 + \cdots$$

Now, consider the parameters of the non-reheated turbine without or with droop characteristic as discussed in the previous section. The parameters (K_P, T_P, T_T and T_G) variation of 30% and 20% are considered simultaneously for NRTWD and NRTD, respectively. The closed-loop characteristic equation of the system is given by

$$1 + GG_c = 0$$

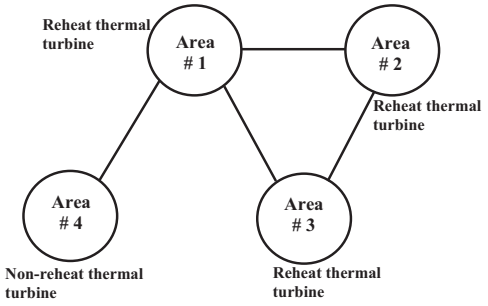

Fig. 19. Simplified diagram of a four area power systems.

The four Kharoitonov polynomials

$$K_1(s) = 357.9498 + 449.4338s + 435.6944s^2 + 54.0864s^3 + 2.5926s^4 + 0.0575s^5$$

$$K_2(s) = 664.7639 + 834.6629s + 234.6047s^2 + 29.1234s^3 + 4.8148s^4 + 0.1067s^5$$

$$K_3(s) = 664.7639 + 449.4338s + 234.6047s^2 + 54.0864s^3 + 4.8148s^4 + 0.0575s^5$$

$$K_4(s) = 357.9498 + 834.6629s + 435.6944s^2 + 29.1234s^3 + 2.5926s^4 + 0.1067s^5$$

for NRTWD and

$$K_1(s) = 260.918 + 388.6268s + 130.7567s^2 + 19.8579s^3 + 0.9999s^4 + 0.0126s^5$$

$$K_2(s) = 391.377 + 582.9403s + 87.1711s^2 + 13.2386s^3 + 1.4998s^4 + 0.0188s^5$$

$$K_3(s) = 391.377 + 388.6268s + 87.1711s^2 + 19.8579s^3 + 1.4998s^4 + 0.0126s^5$$

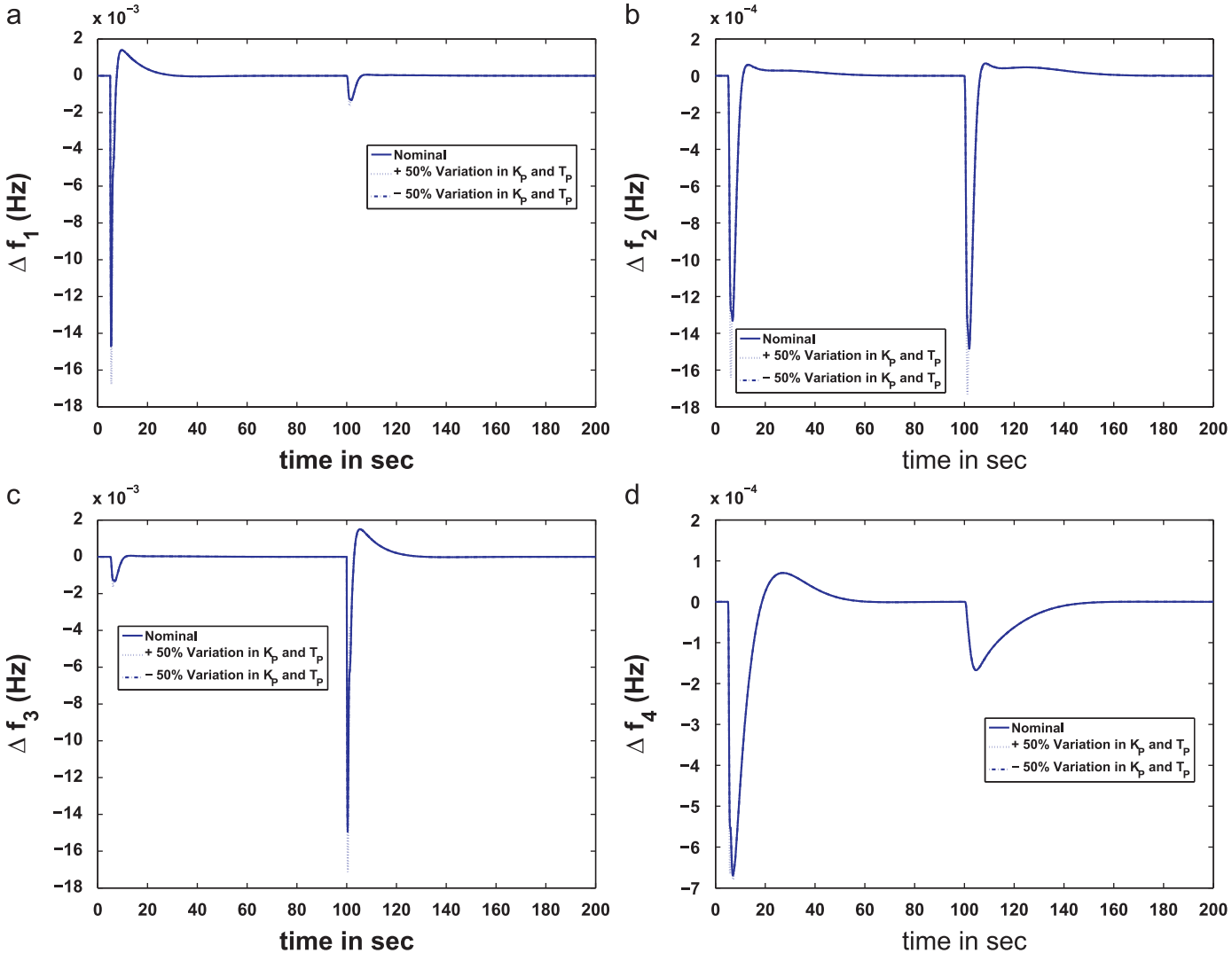

Fig. 20. Frequency deviation for four area power systems: (a) area 1; (b) area 2; (c) area 3; and area 4.

$$K_4(s) = 260.918 + 582.9403s + 130.7567s^2 + 13.2386s^3 + 0.9999s^4 + 0.0188s^5$$

for NRTD.

The coefficients of Kharitonov polynomials for NRTWD and NRTD are checked for Hurwitz condition. It is observed that all the roots of the Kharitonov polynomials (see Tables 2 and 3) have negative real part i.e. all roots are in the left half of the complex plane. From Figs. 16 and 17, it is clear that Kharitonov rectangles move about the origin in counter-clockwise sense in order to have the monotonic phase increase property of Hurwitz polynomials. The graph is zoomed to show what is happening in the neighborhood of the point (0,0). Since the origin is excluded from the Kharitonov rectangles (Figs. 16 and 17) it is concluded that the closed-loop control system is robustly stable. By following a similar procedure as above the robustness analysis considering parametric uncertainties in the plant parameters for RTWD and RTD can be checked.

4. Multi-area power system

A multi-area power system comprises areas that are interconnected by high voltage transmission lines or tie-lines. The trend of frequency measured in each control area is an indicator of the trend of the mismatch power in the interconnection and not in the control area alone [32]. In case of a decentralized power system, area frequency and tie-line power interchange vary as power load demand varies randomly. The objectives of decentralized LFC are to minimize the transient deviations of these variables and to ensure their steady state errors to be zero. When dealing with the LFC problem of power systems, unexpected external disturbances, parameter uncertainties and the model uncertainties pose big challenges for controller design. For N control areas (Fig. 18), the total tie-line power change between area 1 and other areas is

$$\Delta P_{tiei} = \sum_{\substack{j=1 \\ j \neq i}}^{N} \Delta P_{tieij} = \frac{1}{s}\left[\sum_{\substack{j=1 \\ j \neq i}}^{N} T_{ij}\Delta f_i - \sum_{\substack{j=1 \\ j \neq i}}^{N} T_{ij}\Delta f_j\right]$$

The balance between connected control areas is achieved by detecting the frequency and tie line power deviations to generate the area control error (ACE) signal, which is in turn utilized in the control strategy as shown in Fig. 18. The ACE for each control area can be expressed as a linear combination of tie-line power change and frequency deviation.

$$\mathrm{ACE}_i = B_i\Delta f_i + \Delta P_{tiei} \tag{35}$$

where B_i is the frequency bias coefficient. The LFC system in each control area of an interconnected (multi-area) power system should

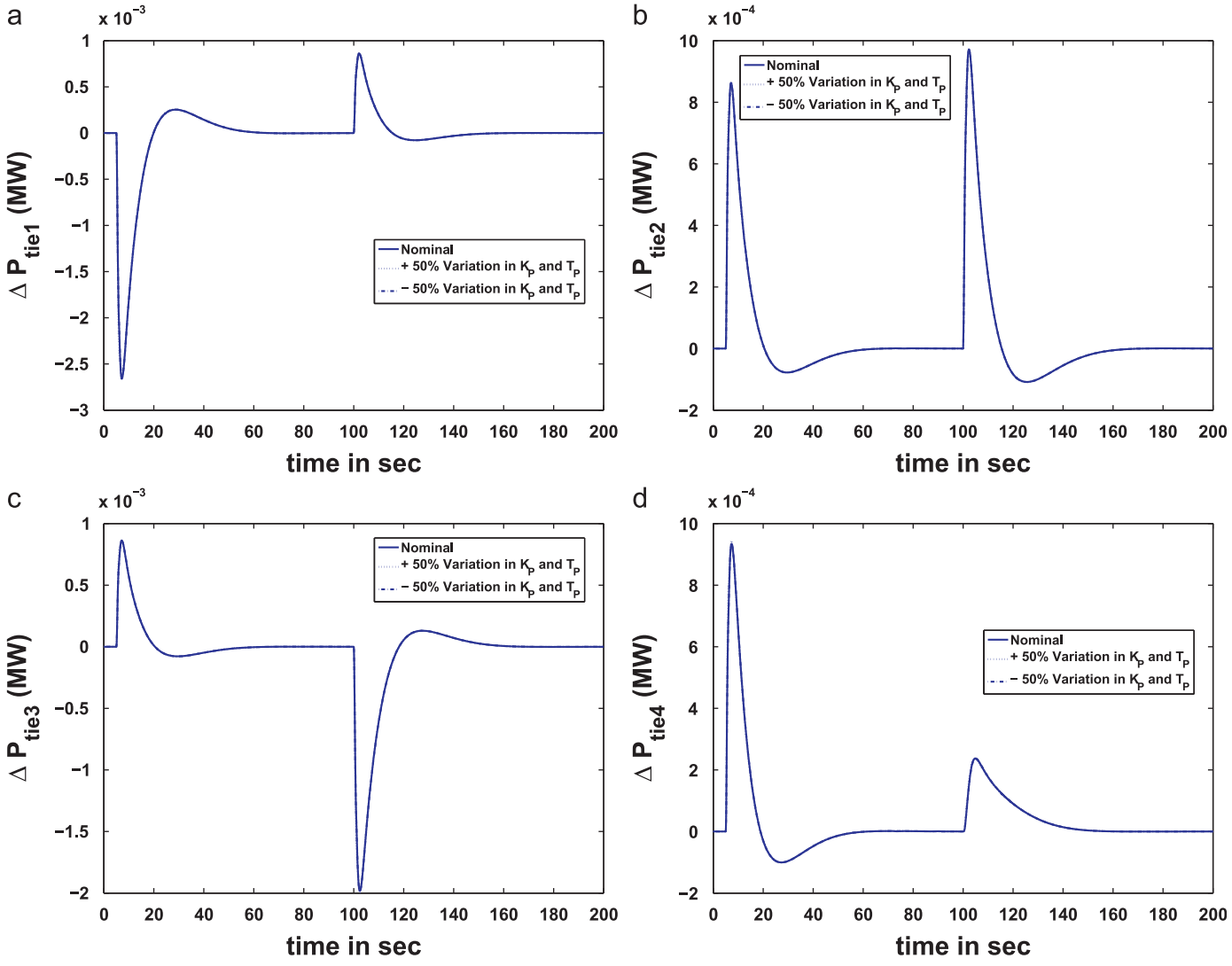

Fig. 21. Tie line power deviation for four area power systems: (a) area 1; (b) area 2; (c) area 3; and (d) area 4.

control the interchange power with the other control areas as well as its local frequency. The plant model for multi-area power system is given by

$$G_i = B_i \frac{G_{gi}G_{ti}G_{pi}}{1+G_{gi}G_{ti}G_{pi}/R_i} \tag{36}$$

For the tuning of multi-area LFC, the same procedure can be followed as in single-area LFC tuning.

4.1. Simulation results for four area power systems

The simplified diagram of a four area power systems is shown in Fig. 19. In the simulation results, area 1, area 2 and area 3 are denoted as the area with reheat unit, and area 4 is denoted as the area with non-reheat unit.

The parameters of the non-reheat and reheat units in different areas are chosen as

Nominal parameters for area 1, area 2 and area 3: $T_{P1} = T_{P2} = T_{P3} = 20$, $T_{T1} = T_{T2} = T_{T3} = 0.3$, $T_{G1} = T_{G2} = T_{G3} = 0.2$, $K_{P1} = K_{P2} = K_{P3} = 120$, $R_1 = R_2 = R_3 = 2.4$, $T_{r1} = T_{r2} = T_{r3} = 20$ and $c_1 = c_2 = c_3 = 0.333$.
Nominal parameters for area 4: $K_{P4} = 120$, $T_{P4} = 20$, $T_{T4} = 0.3$, $T_{G4} = 0.08$, $R_4 = 2.4$.

The synchronizing constants are $T_{12} = T_{23} = T_{31} = T_{41} = 0.0707$ and the frequency bias constants are $B_1 = B_2 = B_3 = B_4 = 0.425$. The identified model for reheat unit with droop characteristic is obtained as $G = 0.9965e^{-0.5s}/(0.72s^2 + 1.7s + 1)$ and that for non-reheat unit with droop is same as that of given in Table 1. By choosing $\lambda = 0.7$ and $\beta = 0.35$, the controller settings for area 1, area 2 and area 3 are $K_c = 1.1895$, $T_i = 1.9090$ and $T_d = 0.5454$. Similarly, the controller parameters for area 4 are $K_c = 1.9822$, $T_i = 0.5242$ and $T_d = 0.1756$ by taking $\lambda = 0.1$ and $\beta = 0.35$.

To show the performance of the decentralized PID controller, a step load $\Delta P_{d1} = 0.01$ is applied to area 1 at $t = 5$ s, followed by a step load $\Delta P_{d3} = 0.01$ to area 3 at $t = 100$ s. Fig. 20 illustrates the frequency errors of the four different areas. Fig. 21 shows the tie-line power errors of the four areas. From the simulation results, it can be seen that the frequency errors, and tie-line power deviations have been driven to zero by proposed controller in the presences of power load changes.

In order to test the robustness of the controller, the variations of the parameters of the non-reheat and reheat units in the four areas are assumed to be $\pm 50\%$ of their nominal values. However, the controller parameters are not changed with the variations of the system parameters. Fig. 20 illustrates the frequency errors of four areas with the variant parameter values. Fig. 21 shows the tie-line power errors of the four areas with the variant parameter values. From the simulation results, it can be seen that despite such large parameter variations, the system responses do not show notable differences from the nominal values. Therefore, the simulation results demonstrate the robustness of proposed controller against system parameter variations. It is observed that the proposed decentralized PID controller achieves better damping for frequency and tie-line power flow deviations in all the four-areas.

5. Conclusion

The LFC characteristics of a single-area power system with non-reheat and reheat turbines have been studied. A relay feedback test has been conducted to estimate the parameters of the power system. The robustness of the LFC is tested using Kharitonov's theorem. The results show that the proposed PID controller with a new structure gives a better performance than reported methods. The proposed method is applied to a four-control area power system and tested with different plant parameters uncertainty scenarios.

References

[1] Kundur P. Power system stability and control. New York: McGraw-Hill; 1994.
[2] Jaleeli N, VanSlyck LS, Ewart DN, Fink LH, Hoffmann AG. Understanding automatic generation control. IEEE Transactions on Power Systems 1992;7(August (3)):1106–22.
[3] Ibraheem, Kumar P, Kothari DP. Recent philosophies of automatic generation control strategies in power systems. IEEE Transactions on Power Systems 2005;20(1):346–57.
[4] Shayeghi H, Shayanfar H, Jalili A. Load frequency control strategies: a state-of-the-art survey for the researcher. Energy Conversion and Management 2009;50:344–53.
[5] Agathoklis P, Hamza MH. Comparison of three algorithms for load frequency control. Electric Power Systems Research 1984;7:165–72.
[6] Aly G, Abdel-Magid YL, Wali MA. Load frequency control of interconnected power systems via minimum variance regulators. Electric Power Systems Research 1984;7:1–11.
[7] Park YM, Lee KY. Optimal decentralized load frequency control. Electric Power Systems Research 1984;7:279–88.
[8] Pan CT, Liaw CM. An adaptive controller for power system load frequency control. IEEE Transactions on Power Systems 1989;4(1):122–8.
[9] Rubaai A, Udo V. An adaptive control scheme for load-frequency control of multiarea power systems Part I. Identification and functional design. Electric Power Systems Research 1992;24:183–8.
[10] Rubaai A, Udo V. An adaptive control scheme for load-frequency control of multiarea power systems Part II. Implementation and test results by simulation. Electric Power Systems Research 1992;24:189–97.
[11] Rubaai A, Udo V. Self-tuning load frequency control: multilevel adaptive approach. IEE Proceedings: Generation, Transmission and Distribution 1994;141(4):285–90.
[12] Chang C, Fu W. Area load frequency control using fuzzy gain scheduling of PI controllers. Electric Power Systems Research 1997;42:145–52.
[13] Ray G, Prasad A, Prasad G. A new approach to the design of robust load-frequency controller for large scale power systems. Electric Power Systems Research 1999;51:13–22.
[14] Hosseini S, Etemadi A. Adaptive neuro-fuzzy inference system based automatic generation control. Electric Power Systems Research 2008;78:1230–9.
[15] Khodabakhshian A, Edrisi M. A new robust PID load frequency controller. Control Engineering Practice 2008;16:1069–80.
[16] Khodabakhshian A, Hooshmand R. A new PID controller design for automatic generation control of hydro power systems. Electrical Power and Energy Systems 2010;32:375–82.
[17] Tan W. Unified tuning of PID load frequency controller for power systems via IMC. IEEE Transactions on Power systems 2010;25(1):341–50.
[18] Tan W. Tuning of PID load frequency controller for power systems. Energy Conversion and Management 2009;50:1465–72.
[19] Tan W. Decentralized load frequency controller analysis and tuning for multi-area power systems. Energy Conversion and Management 2011;52:2015–23.
[20] Tan W, Xu Z. Robust analysis and design of load frequency controller for power systems. Electric Power Systems Research 2009;79:846–53.
[21] Dong L, Zhang Y, Gao Z. A robust decentralized load frequency controller for interconnected power systems. ISA Transactions 2012;51(3):410–9.
[22] Panda RC. Synthesis of PID tuning rule using the desired closed-loop response. Industrial and Engineering Chemistry Research 2008;47:8684–92.
[23] Balaguer P, Alfaro V, Arrieta O. Second order inverse response process identification from transient step response. ISA Transactions 2011;50(2):231–8.
[24] Mei H, Li S. Decentralized identification for multivariable integrating processes with time delays from closed-loop step tests. ISA Transactions 2007;46(2):189–98.
[25] Natarajan K, Gilbert A, Patel B, Siddha R. Frequency response adaptation of pi controllers based on recursive least-squares process identification. ISA Transactions 2006;45(4):517–28.
[26] Majhi S. Relay based identification of processes with time delay. Journal of Process Control 2007;17:93–101.
[27] O'Dwyer A. Handbook of PI and PID controller tuning rules. 2nd editionImperial College Press; 2006.
[28] Zhou K, Doyle JC. Essentials of robust control. Upper Saddle River: Prentice Hall; 1998.
[29] Morari M, Zafiriou E. Robust process control. Englewood Cliffs: Prentice Hall; 1989.
[30] Chapellat H, Dahleh M, Bhattacharyya SP. Robust stability under structured and unstructured perturbations. IEEE Transactions on Automatic Control 1990;35(10):1100–8.
[31] Bhattacharyya SP, Chapellat H, Keel LH. Robust control: the parametric approach. Prentice Hall; 1995.
[32] Bevrani H. Robust power system frequency control. Springer; 2009.